Deutscher Luft- und Raumfahrtkongress 2008
DocumentID: 81252

# AUTOMATED AERODYNAMIC OPTIMISATION OF A TRANSONIC COMPRESSOR STAGE BY APPLICATION OF NON-AXISYMMETRIC ENDWALLS

S. Reising, H.-P. Schiffer
Chair of Gas Turbines and Aerospace Propulsion
Technische Universität Darmstadt
Petersenstraße 30, 64287 Darmstadt
Germany

T. Hildebrandt, P. Thiel
NUMECA Ingenieurbüro
Türkeistraße 11, 90518 Altdorf b. Nürnberg
Germany

## SUMMARY

In the last few decades the development of axial aircraft compressors has led to extremely high stage loadings to reduce the entire engine size and weight. Stage loading is recognized to be the single most important design decision due to its influence on the overall performance and on the engine size. However, this trend also promotes several disadvantages as e.g. the risk of separation on the suction side and higher secondary flow due to the increased circumferential static pressure gradient in the blade channel.

The application of non-axisymmetric endwalls is one approach to reduce blade loading in the hub region and to control endwall flow with the main objectives of increasing the component efficiency and the total pressure ratio. The challenge hereby is to find the optimal non-axisymmetric endwall shape which results in the largest benefit in performance. In this paper an approach is presented to find a fully 3D endwall geometry that satisfies the mentioned requirements. This approach is based on an optimization chain using the commercial CFD Software FINE™/Turbo and FINE™/Design3D.

This procedure is applied on the known Configuration I of the Darmstadt Transonic Compressor, limited to the hub endwall of the stator. The numerical results show a high benefit in overall performance resulting in a rise in stage efficiency of 1.65% and a slight improvement in total pressure ratio.

## 1. INTRODUCTION

The design process of modern turbomachinery is a complex and time-consuming task involving many different objectives and constraints. Until the 80s, this was even more challenging since almost the entire design had to be done analytically by the engineer. Fortunately, computational power has increased enormously over the last decades helping the designer to define advanced blade geometries, compute the flow field inside the blade channels and the mechanical stresses in the solid parts of the machine. This is even more important when it comes to the design of non-axisymmetric endwalls in transonic compressors. Although a lot of research on this topic has been done for turbines [1,2,3], the knowledge of design rules for the applications in compressors is very limited. As a consequence, designers often start from an existing axisymmetric contour and try to adapt and improve it based on trial and error. However, mostly only a limited amount of prototypes are affordable due to restricted budgets and the request for very short design time schedules.

Although CFD Software is getting more and more accurate, fast and user friendly it normally does not provide algorithms which are able to automatically optimise the performance of a new geometry. Due to the above mentioned restrictions, designers cannot take full advantage of the huge potential and amount of information that is provided by CAD, CFD and structural codes.

The optimisation problems associated to turbomachinery design often involve many constraints and a large set of parameters which result in objective functions presenting many extrema. It is well known that optimisation methods based on gradients techniques are efficient in terms of convergence rate but do not guarantee to find the global optimum [4]. In contrast, genetic algorithms offer the advantage of enhancing the probability of reaching the global optimum but, unfortunately, may require thousands of iterations [5]. Their coupling with a three-dimensional Navier-Stokes solver is time-consuming and thus difficult within the framework of an industrial design process.

The major idea of the optimisation approach [6] to be presented in this paper is that the evaluation of the successive designs is performed using an artificial neural network instead of a flow solver permitting to use the genetic algorithm in an efficient manner. The accuracy of the optimisation depends on the knowledge of the neural network which is fed by design examples stored in a database.

The presented design exercise demonstrates the application of an optimisation strategy in order to design of a non-axisymmetric hub endwall of a transonic compressor. As a test case, the known Configuration I of the Darmstadt Transonic Compressor [7,8] is used.

## 2. THE FINE™/DESIGN 3D ENVIROMENT

### 2.1. General Principle of the Method

The idea of the presented method, of which a flow chart is shown in Figure 1, is to accelerate the design of new endwall contours by using the knowledge acquired during the previous designs of similar contours.

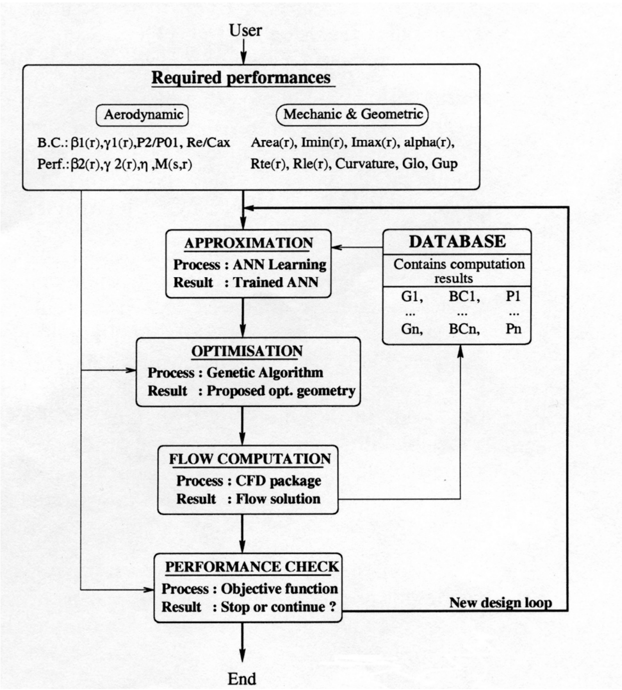


Figure 1. Endwall design algorithm [9]

The entire optimisation process consists of the following steps:

1) Parameterisation of the geometry to reduce the geometrical degrees of freedom
2) Creation of a meshing template for the grid generator
3) Definition of the free and fixed geometrical parameters
4) Generation of the initial databases based on CFD simulations of arbitrary geometric samples
5) Definition of the optimisation goals
6) Run of the optimisation by means of the artificial neural network, based on a self-learning algorithm
7) Performance check to compare the current sample with regard to the optimisation goals

The core of the design system is the database containing the results of all Navier-Stokes computations performed during the generation of the initial databases. This database contains three kinds of data for each sample:

- The fluid properties and flow-field boundary conditions used by the Navier-Stokes solver
- The parameters to define each sample's geometry
- Each sample's aerodynamic performance characterised by efficiency, total pressure ratio, the outlet flow angle distributions, mass flow, blade loading and other quantities

After a sufficiently large initial database of arbitrary samples has been generated in an automated way, an iterative procedure is used which is structured as follows:

- A learning process is used to build the neural network based on the examples stored in the initial database. The network contains free parameters that are to be adapted to fit the database samples. A fitting process is performed by back-propagation of the errors. After the mapping of the database samples, the neural network is able to predict the aerodynamic performance of endwall contours that are not part of the database
- The next step is to find a new design by using the mentioned optimisation procedure formed by a genetic algorithm. The performance of this new design is evaluated by means of the trained neural network. To quantify performance, an objective function is used which transfers all user-imposed constraints into a single number. The result of this optimisation is a point which is expected to be close to the global optimum of the design space
- This new geometry is now evaluated by the 3D Navier-Stokes flow solver and added to the database. The comparison of the performance obtained by CFD with the one predicted by the neural network permits to evaluate the accuracy of the network. The new sample's performance is also compared to the design goals. If these have not been achieved another design iteration is started repeating the same process until the optimum geometry has been reached.

As this process proceeds, the database grows after each iteration leading to improvements of the approximate relation and therefore to a better prediction of the real optimum. The key is the enrichment of the database in the proximity of the optimum design while the database in the less interesting areas of the design space remains relatively coarse. An additional advantage of this method is that a database, once generated, can be reused if the design objectives or constraints have been modified for another optimisation. The CPU cost of each iteration mainly depends on the 3D Navier-Stokes calculation, whereas the cost of the optimisation features is much smaller in the dimension of 5% of a CFD simulation.

## 2.2. The Parametric Blade Modeller AutoBlade™

The geometry parameterisation is a critical element in the success of any shape optimisation method. The parameterisation should be able to generate a large variety of physically realistic shapes with as few design variables as possible while providing smooth aerodynamic shapes.

AutoBlade™ is a parametric geometry modeller specific for turbomachinery applications. Designers usually work by generating two-dimensional blade sections which are then stacked along the blade span to obtain the three-dimensional blade geometry. AutoBlade™ offers a number of design modes for the two dimensional blade sections. A suitable one in the case of axial compressors is to generate a camber curve and to add two additional construction curves for the blade's suction and pressure side respectively.

In the example to be presented here, also the endwalls had to be parameterised. As tools, Bezier, B-spline or C-spline curves are available. AutoBlade™ also provides the possibility to analyse the 3D blade shape by computing quantities such as blade thickness, momentum of inertia and curvature at different locations. Afterwards, it is possible to include these quantities in the objective function.

Finally, the variable and fixed geometry parameters are to be chosen. Since only the hub geometry of the stator was to be modified, all parameters except the ones of the non-axisymmetric endwall were kept constant.

## 2.3. The Grid Generation with AutoGrid™

AutoGrid™ is an automatic meshing system for turbomachinery applications developed to ease pre-processing for numerical computations on such configurations. It contains many useful features to enable the user to create meshes for a large range of gas turbines, fans and compressors applications (e.g. Turbofan, Turboprop, axial or centrifugal, single or multistage). The available topologies lead to block-structured grids of high quality.

A big advantage is the possibility to work with meshing templates, i.e. to define mesh properties as grid point distribution, tip clearance etc. and apply them on other configurations by using the template. This is particularly important concerning an optimisation due to the geometry modification of each iteration. First of all, a mesh must be generated for the parameterised initial geometry with a grid quality as high as possible to avoid poor grid qualities afterwards being possible to appear due to the desired geometry modifications. In a multistage project, as described here, the rotor and stator are to be meshed separately in two projects since it is only possible to parameterise and modify one blade row (either rotor or stator) within the FINE™/Design 3D environment. As the project is focused on the contouring of the stator hub, the stator mesh has to be generated for each iteration by means of the template. The rotor mesh remains the same and can, once generated, be used for every modified design. The rotor is then connected to the new stator in a script and the stator is optimised within the full stage environment in order to account for any possible upstream effect of the stator onto the rotor.

## 2.4. The Approximate Model

The basic principle of the method is to build an approximate model of the original analysis problem. This model can then be used inside an optimisation loop instead of the original model. In this way the performance evaluation by the approximate model is not costly because no CFD simulation is needed for this purpose. Thus, the number of performance evaluations executed by the model for the optimisation is no longer critical. Among the large number of possible techniques able to construct such a model, an artificial neural network (ANN) has been selected. Even though the initial motivation for the development of the ANN was to establish computer models being able to imitate certain brain functions, ANN can also be considered as a powerful multi-dimensional interpolator.

Artificial neural networks are non-linear models that can be trained to map functions with multiple inputs and outputs. The ANN consists of series of layers [10], each of them being composed of a given number of 'nodes' (Figure 2). The first input layer connects all inputs (i.e. the non-axisymmetric endwall geometry and the constraints) to the network whereas the last output layer produces the outputs (i.e. the aerodynamic performance). All inputs of a layer are connected to all nodes of this layer through weighting factors. The summation of all the contributions with a corresponding additional bias value is introduced in a sigmoidal function F where the output of each node is given by:

(1) $$a_n(i) = F\left\lfloor \sum_{j=1}^{S(n-1)} W_{ij} a_{n-1}(j) + b(i) \right\rfloor = F[i_n(i)]$$

The training of the neural network consists of finding the components of the weight matrices that lead to the best reproduction of the examples stored in the database trying to minimise the error that the ANN produces on the database samples:

(2) $$E^l = \tfrac{1}{2} \sum_{j=1}^{nout} (d_j^l - a_j^j)^2$$

Here, $d_i$ and $a_i$ represent the database and the corresponding ANN values of the first output for a given sample l. This optimisation problem can be solved by using a gradient method, which is usually referred to as the back-propagation approach. The derivatives of the error regarding the weight factors are expressed which permits to calculate iteratively the weight and bias components modifications to eliminate the error.

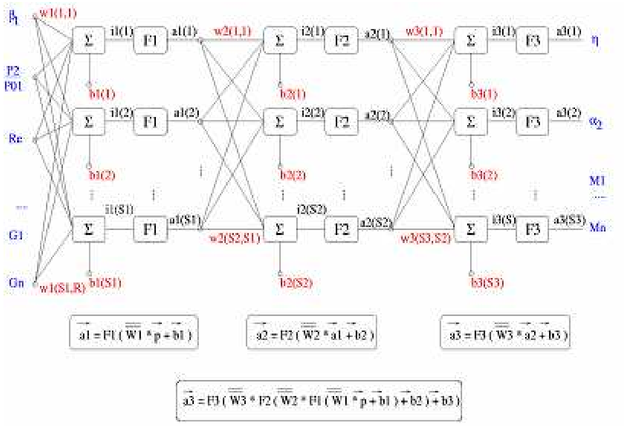


Figure 2. Schematic view of an ANN

### 2.5. The Optimisation Algorithm

The goal of the optimisation is to find the minimum of the objective function using the simplified analysis model. In this context, an essential issue is the robustness of the numerical optimisation algorithm. The choice of the optimisation algorithm is mainly based on the following two considerations:

- Many local optima may exist in the design space and therefore a global optimisation technique is required.
- The evaluation of the performance using the approximate model is very fast (a few ms). Consequently, the number of needed function evaluations is now of far less importance than if a detailed CFD computation was needed at each step.

Based on the first consideration, the straightforward application of numerical optimisation techniques that rely on derivatives is questionable because of its local properties. In contrast, stochastic techniques such as the genetic algorithm or simulated annealing are global optimisation methods that do not get stuck in a local minimum and thus offer an alternative to conventional gradient methods which, however, has the advantage of a fast function evaluation. Genetic algorithms were designed by Holland in the 70s and improved by Goldberg in the 80s [4].

A genetic algorithm is summarised as follows. An initial population is generated by randomly selecting individuals in the whole design space. Then, pairs of individuals are selected from this population based on their objective function values. The performance of an individual is evaluated by its fitness. After that, each pair of individuals undergoes a reproduction mechanism to generate a new population in such way that fitter individuals will spread their genes with higher probability. The children replace their parents. As this proceeds, inferior traits in the pool die out due to their lack of reproduction. At the same time, strong traits tend to combine with other strong traits to produce children who perform even better.

### 2.6. The Objective Function

Among the design objectives of a detailed aerodynamic shape optimisation, efficiency is only one of the many considerations. A good design must also satisfy the mechanical, manufacturing and aerodynamic constraints. In the presented case, this may be the outlet flow angle profile, the throat area due to the contouring's impact on the cross section, and the pressure loss coefficient. The optimisation problem can be seen as the minimisation of an objective function in function of several variables (geometrical parameters) subject to several constraints (mechanical, manufacturing and aerodynamic constraints), the objective function and the constraints being non-linear. The general approach for solving this problem is to transform the original constrained minimisation problem into an unconstrained one by converting the constraints into penalty terms that will increase when the constraints are violated. Summing up all penalty terms and the original objectives then creates a pseudo-objective function

(3) $$OF = \sum_{penalties} w * P \, .$$

Here, w is weighting factor that the user has to associate to each penalty. One can notice that the difference between the actual value V and the required one $V_{req}$ is divided by a reference value $V_{ref}$, in order to provide all terms with a similar order of magnitude. Depending on the type of constraint, the penalties will have the following formulations:

- Upper Bound:
  If $V > V_{req}$ then

(4) $$P = \left(\frac{V - V_{req}}{V_{ref}}\right)^x \text{ else P=0}$$

- Lower Bound:
  If $V < V_{req}$ then

(5) $$P = \left(\frac{V_{req} - V}{V_{ref}}\right)^x \text{ else P=0}$$

- Equality constraint:

(6) $$P = \left(\frac{fabs(V - V_{req})}{V_{ref}}\right)^x$$

The optimisation technique that is adopted in FINE™/Design3D can be considered as single objective since all objectives and constraints are put together into one single function. Weighting functions are associated to the different constraints allowing the user to reflect the levels of priority into the optimisation. According to this it is evident that different values for the weighting factors will lead to different solution, i.e. different optimum geometries.

## 3. OPTIMISATION OF THE TRANSONIC COMPRESSOR STAGE

The optimisation method which has been described in the previous chapter was applied on the Configuration I of the Darmstadt Transonic Compressor, limited to the hub endwall of the stator stage as a first step. It was focused on a single-point optimisation of the design point. In order to find this point a speed line was calculated at design speed of 20000 rpm (see Figure 8) which led to a peak efficiency of 85.43% at a mass flow rate of 15.09kg/s. The compressor specifications are shown in TAB 1 whereas the flow angles are the design flow angles and not the calculated ones.

| Quantity | Value | Units |
|---|---|---|
| Blades Rotor | 16 | [ - ] |
| Blades Stator | 29 | [ - ] |
| Mass Flow | 15.09 | [ kg/s ] |
| Isentropic Efficiency (Stage) | 85.43 | [ - ] |
| Total Pressure Ratio | 1.46 | [ - ] |
| Deviation Angle Stator Exit | 0 | [ °] |
| Meridional Angle Stator Exit | 0 | [ °] |
| Tip Speed | 400 | [ m/s ] |

TAB 1. Compressor specifications (Design Point)

## 3.1. The Parametric Model

### 3.1.1. Parameterisation of the Stator Blade

Since the optimisation of the blade was not the objective to be accomplished and its shape was to keep fixed during the process, more attention was paid on the best possible agreement between the original and the parameterised blade geometry than on a high number of parameters what might have been a benefit in a blade optimisation. For the camber curve, 9 parameters with a contribution factor of 1.4 were used. Both the pressure and the suction side were parameterised with 8 points and a stretching factor of 1.1 having the leading edge as a reference point. After the fitting, the unavoidable deviations between the original and the fitted geometry have to be evaluated. As it can be seen in Figure 3, the main shape of the blade is met very well. However, there were slight differences in the region around the leading edge due to the fact that the stator has been designed in a more traditional way of adding a rounded leading edge to the blade contour, while AutoBlade™ by default creates a blade shape with no second order discontinuities.

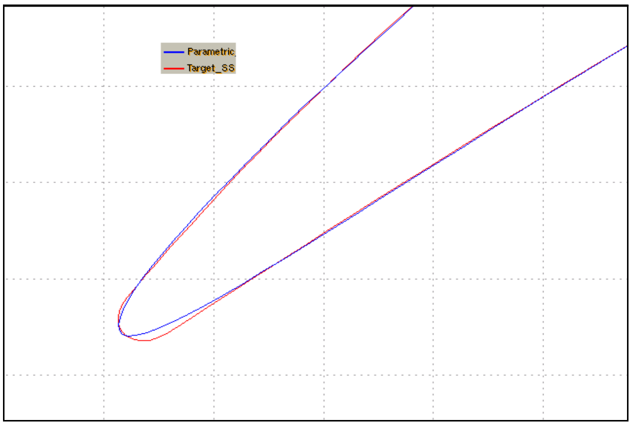


Figure 3. Geometrical difference between original and fitted blade shape at the leading edge

A second speed line was calculated with the parametric model showing no observable differences in efficiency and total pressure ratio in comparison to the original geometry. To investigate the geometrical deviation more in detail, the boundary layer and the blade loading around the leading edge were analysed which, again, did not show any noticeable disagreements. Thus, the parametric model was assumed to satisfy the required accuracy compared to the original one.

### 3.1.2. Parametrisation of the Stator Hub Endwall

AutoBlade™ provides two possibilities, namely the method 'Across Channel' and the method 'Along Channel', to parameterise endwall geometries. The method 'Across Channel' builds cuts perpendicular to a channel line which corresponds with the camber curve. This method is limited to the blade channel area only. The method 'Along Channel', which is generally more suitable for axial turbomachinery applications, consists in building the cuts along a virtual stream line. The virtual streamline is also aligned with the blade camber curve. However, using this method, the cuts may extend outside the blade channel by a distance the user has to define. In the presented case of the Darmstadt Compressor the parameterised area started upstream of the leading edge by 10% of the blade channel's meridional extension (see Figure 4). Within the blade channel, only the first third of the area was parameterised. The reason for that was the huge separation zone on the suction side in the rear part of the stator which was detected during the analysis of the initial design (see Figure 11 in chapter 4). This separation bubble was suspected to drive the optimiser to totally unrealistic configurations which one would not be able to manufacture. Therefore, the perturbation area was limited to the part of the blade channel where the separation had not begun to develop yet.

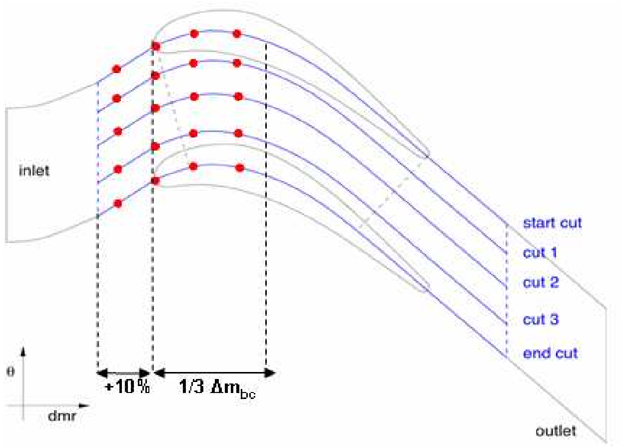


Figure 4. Cut definition for method 'Along Channel'

The blade channel was divided into 5 cuts, each with a distance of 25% of the blade channel width to the next one. Along the cuts, a uniform distribution of 4 parameters was selected. In total, this would have led to 20 free parameters if the perturbation area had been restricted to the blade channel. Since the cuts extended outside the blade channel the start and the end cuts had to be identical to ensure geometrical continuity. Thus, the number of free parameters for the optimisation was reduced to 16. A guide value for the initial database is that the database should contain twice to three times as many valid samples as there are parameters to be varied resulting in approximately 40 samples needed for the example presented here.

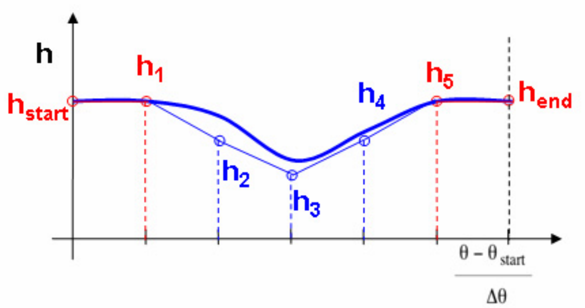


Figure 5. Circumferential perturbation law for the blade channel

In circumferential direction, the user can additionally choose the option of slope continuity which was also done here. The additional values $h_1$ and $h_5$ (see Figure 5) are automatically managed by the algorithm and cannot be accessed by the user. For the optimisation, all parameters were allowed to vary between -2.5mm and 2.5mm in vertical direction.

### 3.2. Meshing of the Initial Geometry

Prior to launching an optimisation, an analysis of the initial geometry has to be performed. This is of crucial importance to ensure the robustness of all meshing parameters over a wide range of possible geometry modifications which may occur in unforeseeable combinations of free parameters. That way, unacceptable high degradation of mesh quality can be prevented.

Both rotor and stator were meshed with a 4HO topology. The rotor mesh consisted of approximately 1.36 million grid points with a minimum skewness of 36 degrees. The stator mesh of the initial geometry had a size of around 800 000 points with a minimum skewness of 54 degrees. This high value in skewness was possible due to using the 'High Staggered Blade Optimisation' menu. When using this option, as shown in the upper block no. 5 in Figure 6, the grid points of the outlet patch do not correspond with the inlet patch any longer but with the connection to the block below (red lines in Figure 6). The H upper block then becomes a C-block. Moreover, a matching periodic boundary condition was used for the blade-to-blade connection to minimise the numerical error.

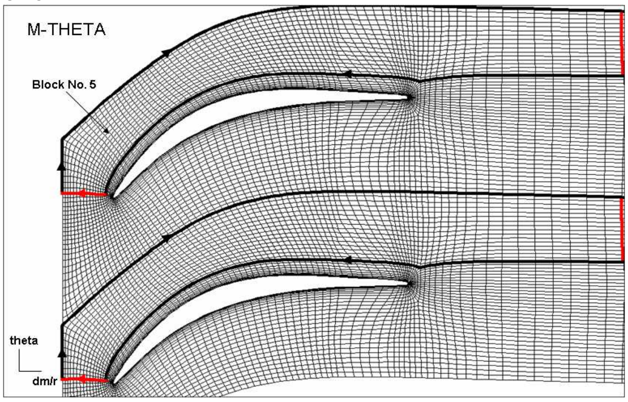


Figure 6. Blade-to-blade mesh with high staggered option and matching connection

The robustness of the mesh topology had been checked prior to the optimisation by an automated meshing run of more than 50 randomly generated endwall profiles, checking all important grid quality parameters. The minimum mesh skewness was in no case less than 38 degrees. Also, all other parameters like aspect ratio and expansion ratio were uncritical.

### 3.3. Design of the Non-Axisymmetric Endwalls via Optimisation

Before launching the optimisation to find the ideal shape of the non-axisymmetric hub endwall, the objectives and the restrictions had to be defined.

- The first objective was to increase the isentropic efficiency of the stage. The target value was set to 1. This is always a sensible assumption although this idealised value will never be reached. However, samples with higher efficiency will receive a lower penalty than the ones with lower efficiency.
- The second objective was to increase the total pressure ratio. Since no work is put into the fluid in a stator, an increase in isentropic efficiency is always connected with a raise in total pressure ratio if the fluid enters the stator at the same conditions in both cases. Therefore, no penalty was set for the total pressure ratio because this would have meant only to duplicate the first objective.
- Although no impact of the stator optimisation on the upstream rotor flow was expected, the isentropic efficiency of the rotor (i.e. the flow parameters at the rotor-stator-interface were taken as outlet values) was monitored, also to ensure constant inlet conditions at the stator inlet as described above.
- The objective was to minimise the total pressure loss coefficient of the stator expressed by the mass-weighted integral of

$$CP_{stator} = \frac{p_{tot\_inlet}(r) - p_{tot\_outlet}(r,\varphi)}{\bar{p}_{dyn\_inlet}} \quad (7)$$

  Even though this is also connected to the first objective, the main focal point was on the spatial distribution of the pressure loss. Thus, only a small weighting factor was set for this penalty.
- The last objective was to approach the 1-dim. outlet flow, intended in the original design. Therefore, both the deviation angle and meridional angle were analysed by terms of penalties. The deviation angle, especially the distribution close to the endwalls, can also be seen as an indicator for secondary flows. Due to lower velocities in the boundary layers at the endwalls, the radial equilibrium between the centrifugal force and the force of the circumferential static pressure gradient is disturbed and a cross flow is generated having a direct impact on the deviation angle.

The optimisation was intended to be carried out at a constant mass flow rate, i.e. at 15.09kg/s (design point) to remain at the same operating point throughout the whole procedure. A change of the velocity profiles at the stator inlet was intended to be avoided which, in turn, would have had an impact on the velocity triangles at the leading edge resulting in difficulties for the comparison between the results of the initial and optimised geometry.

- To fulfil this requirement the inlet area had to be kept constant by defining a geometrical restriction. A change of the cross section would lead to a change in the axial velocity component and therefore to an alternation of the velocity triangles. An additional penalty was set on this geometrical restriction

Hence, the entire objective function added up to:

$$OF = w_\eta P_\eta + w_{\eta rot} P_{\eta rot} + w_{cp} P_{cp} + w_\alpha P_\alpha + w_A P_A \quad (8)$$

In TAB 2, all required and reference values, as well as the weighting factors are shown. The exponents were set to be 2 for all penalty terms. Although only 40 samples would have been necessary for the initial database, a total of 60 samples was generated. Each sample was automatically checked in order to ensure robust convergence. Only if a sample passed all convergence criteria (mass flow conservation, level of residual reduction, no fluctuations in computed efficiency) it was allowed to enter the database. In order to speed up the generation of the database, a number of independent database generation processes were launched on 12 processors. Independency of the individual databases was guaranteed by providing different starting conditions for each database. All valid samples from the different databases were then merged into the final one which served as the initial database for the optimisation. Due to some invalid samples concerning the mentioned specifications, 44 samples remained for the initial database.

| Penalty | $V_{req}$ | $V_{ref}$ | W |
|---|---|---|---|
| Efficiency Stage | 1 | 1 | 10 |
| Efficiency Rotor | 89.99 | 89.99 | 2 |
| Flow Angle [°] | 0 | 1 | 2 |
| $CP_{Stator}$ | 0 | 1 | 2 |
| Throat Area [$m^2$] | 0.00197 | 0.00197 | 10 |

TAB 2. Parameters for the objective function

Based upon this database, the optimisation process was started. The convergence history of the optimisation procedure is shown in Figure 7. One can observe that the error between the neural network predictions and the CFD results decreases. The ANN gets better with ongoing time, gaining more information after each sample. Both curves finally converge after some 30 iterations.

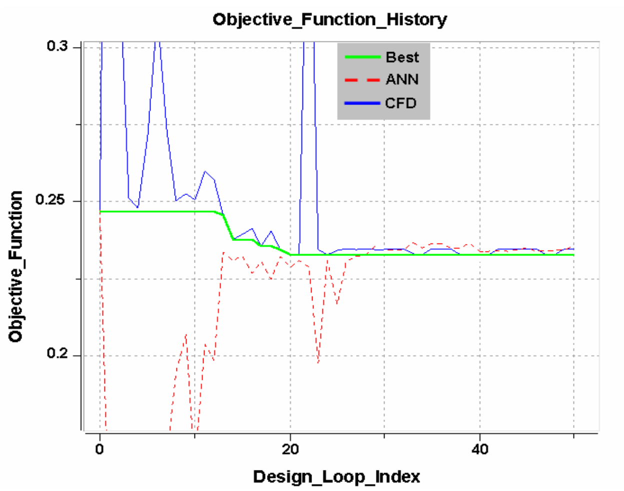


Figure 7. Convergence history of the objective function

The main reduction of the objective function takes place between 15 and 20 iterations with only small improvements thereafter. Among all the generated samples that were better than the original one, finally, sample no. 47 was chosen to be the best one. Although there were samples with a slightly lower objective function this sample was selected due to its throat area value. A comparison between the integral flow parameters of the original geometry and the optimised one with the designed non-axisymmetric endwall profile is given in TAB 3. A remarkable raise in stage efficiency of 1.65% could be achieved throughout the optimisation. As preliminarily assumed, the increase in efficiency involved a slight gain in total pressure ratio. This was also the case for all samples generated with a higher efficiency during the optimisation. Moreover, one could assure to avoid an influence on the rotor as can be noticed when looking at the rotor efficiency. The change of the throat area in a range of 0.2% was negligible allowing the stator inlet conditions to be considered identical to the ones from the initial geometry.

| Parameter | Initial Geom. | Optimised Geom. |
|---|---|---|
| Efficiency Stage | 85.43 | 87.08 |
| Efficiency Rotor | 89.99 | 89.99 |
| $\pi_{tot}$ | 1.47 | 1.48 |
| Flow Angle [°] | 1.57 | 0.90 |
| $CP_{Stator}$ | 0.089 | 0.057 |
| Throat Area [$m^2$] | 0.00197 | 0.001966 |

TAB 3. Comparison of the integral flow parameters

The decreasing deviation angle at the stator outlet is evidence to suggest that the cross flow has also been reduced.

## 4. ANALYSIS OF THE RESULTS

In Figure 8 one can notice that the optimisation did not only lead to improvements for design conditions but also for the entire speed line. Moreover it shows that it is reasonable to carry out the optimisation at constant mass flow trying to keep the throat area constant by the application of a penalty. The characteristic line therefore did not experience a shift along the x-axis what would have made a comparison quite difficult due to different capacities. Figure 9 shows the surface subsidence of the non- axisymmetric endwall.

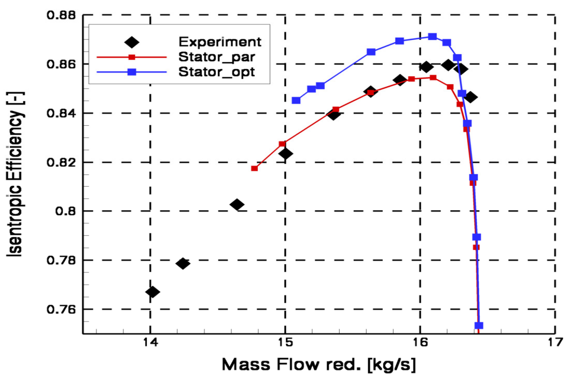


Figure 8. Speed line comparison between parameterised and original geometry

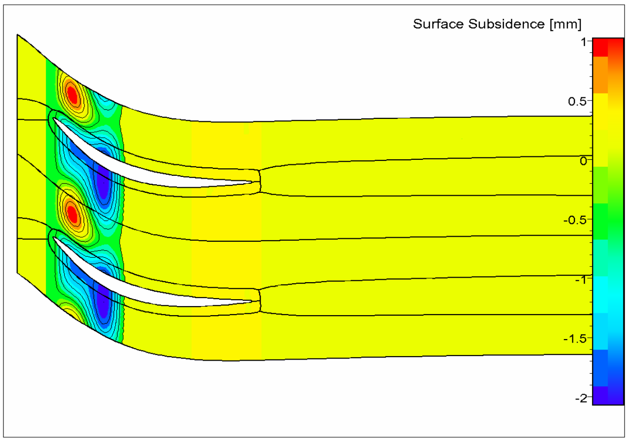


Figure 9. Surface subsidence of stator hub in mm

Between the middle of the blade channel and the pressure side, the optimisation led to convex curvature involving an acceleration of the flow and a reduction in static pressure, what is also indicated in the 3D view of the endwall profile in Figure 10. On the other hand, the contour plot of the endwall shows a concave curvature at the suction side which decelerates the flow increasing the static pressure like in a diffuser.

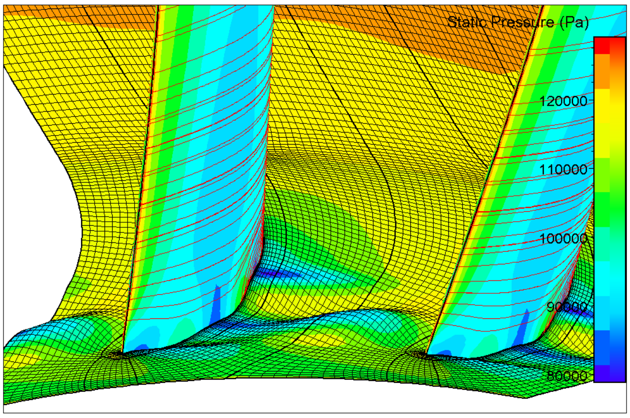


Figure 10. Static pressure distribution on endwall

Having a closer look at the flow characteristics at design conditions, it becomes clearly apparent that the major part of the improvement results from the decrease of the separation zone. Figure 11 displays the suction side of the initial stator showing a huge separation bubble reaching from the hub to approximately 30% channel height. This separation area even enters far into the flow field, indicated by a recirculation area as visible at 5% channel height in Figure 12. Both phenomena result in an enormous loss in total pressure, indicated by the total pressure contours in both graphics mentioned.

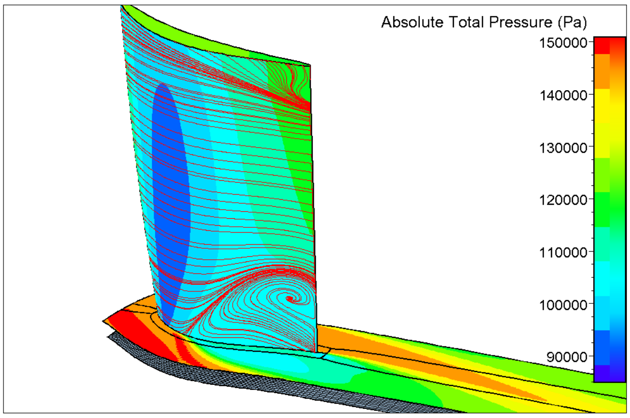


Figure 11. Separation zone of original geometry

Figure 13 shows once again the radial and circumferential extension of the separation zone at the stator outlet. For the optimised design this separation region is by far less pronounced. According to the streaklines on the blade surface in Figure 14, its radial extension is limited to approximately 10% relative channel height. The recirculation zone in the blade channel has been completely eliminated (see Figure 15) leaving only a small zone close to the trailing edge. This leads to a total pressure distribution that is of a far higher level and more homogenous at the stator outlet (see Figure 16). Similar results have been also observed by other authors [11]. According to the evaluated charts, the hub contouring most likely has no influence or at least a negligible one on the flow behaviour in the shroud region.

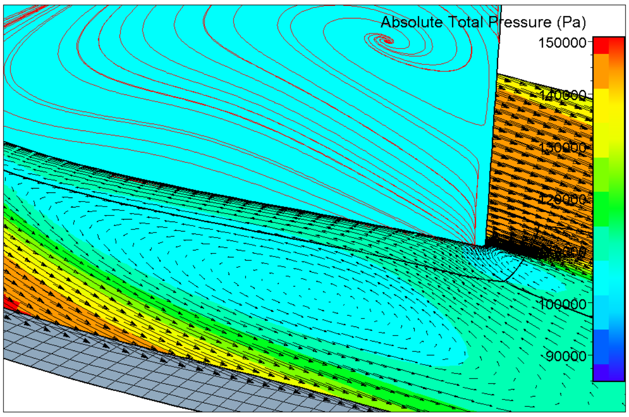


Figure 12. Recirculation at 5% channel height (original geometry)

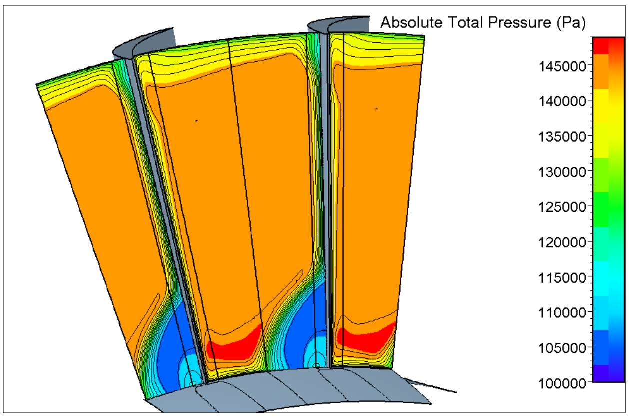


Figure 13. Distribution of $p_{tot}$ at stator exit – original geometry

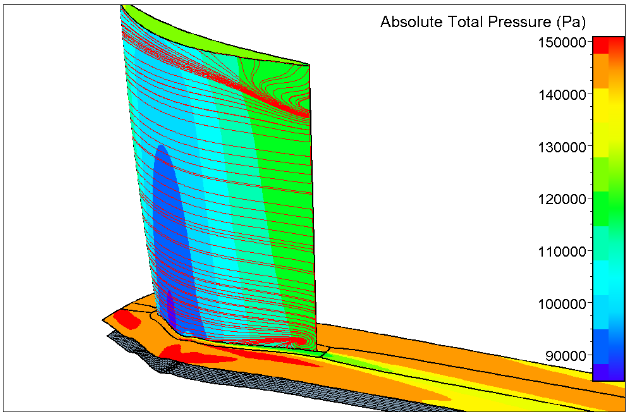


Figure 14. Reduced separation zone of optimised geometry

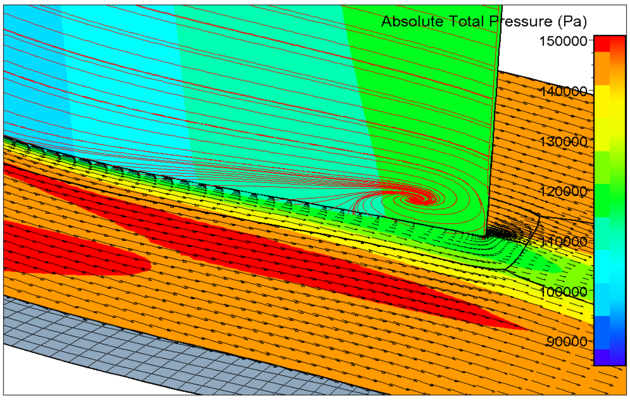


Figure 15. Prevention of the recirculation at 5% channel height (optimised geometry)

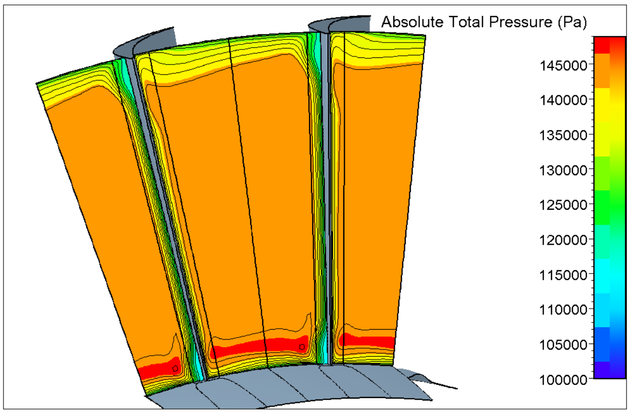


Figure 16. Distribution of $p_{tot}$ at stator exit – optimised geometry

Figure 17 shows the isentropic stator Mach number distribution at 10% channel height. In the case of the original geometry, the flow on the suction side is only decelerated until 40% of the chord length after having reached its maximum velocity. This is due to the separation zone which produces a blockage decreasing the effective cross section for the flow. A further deceleration is not possible.

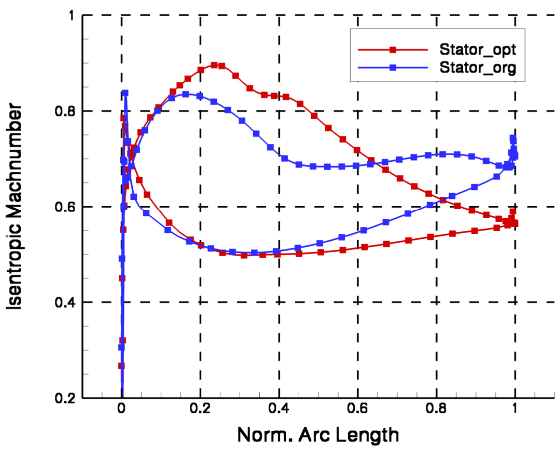


Figure 17. Blade loading at 10% channel height – original and optimised geometry

On the other hand, this reduction of the effective cross section forces the fluid to move to the pressure side with an increase in velocity and as a consequence in a raise of the isentropic Mach number again at the rear part of the pressure side. Unlike the initial geometry, the flow experiences a stronger acceleration on the suction side this time resulting in a higher blade load since the trend of the isentropic Mach number remains comparable to the one of the initial design. However, as the separation with the involved blockage has been reduced dramatically, the flow receives a smoother deceleration after having reached the peak velocity and is further decelerated in the back part of the suction side. This time, the fluid is not forced to move to the pressure side, so that the flow on the pressure side is hardly accelerated after 40% of the chord length.

The last point to be evaluated is the secondary kinetic energy (SKE) at the stator exit. Since the flow downstream of the stator was intended only to consist of an axial component any divergence from an one-dimensional outcoming (i.e. any radial component $V_r$ and any circumferential component $V_t$) flow could be considered as secondary flow leading to the following equation for the SKE:

$$SKE = \frac{1}{2}(V_r^2 + V_t^2) \quad (9)$$

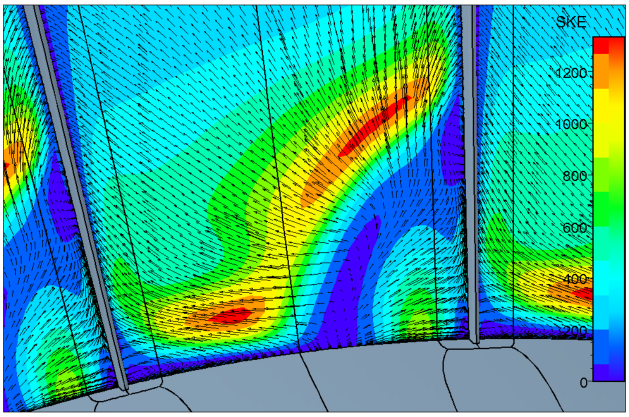


Figure 18. SKE of original geometry at stator exit

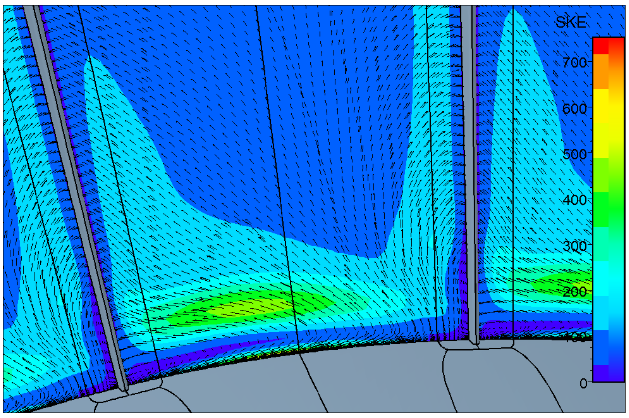


Figure 19. SKE of optimised geometry at stator exit

Figure 18 and 19 show the distribution of SKE and the secondary velocity vectors at stator exit of the initial and optimised geometry respectively. The original design shows a region of extremely high SKE around the separation zone. During the optimisation process the mass weighted integral of SKE at the stator exit plane could be reduced by more than 50 %. Unfortunately, this result does not permit a clear statement about the potential of reducing secondary flows by the application of non-axisymmetric endwalls in the presented example. The huge separation bubble as the main source of loss has probably overlapped the improvements achieved concerning the other loss sources.

## 5. CONCLUSION

An efficient method for constructing non-axisymmetric endwalls using B-splines has been presented and applied to the design of the stator of Configuration I of the Darmstadt Transonic Compressor. The obtained endwall contour led to an improvement in efficiency in the range of 1.65% for the design point. Again, this emphasizes the potential for improving overall stage efficiency in a compressor by using the provided application. The results of the 3D endwall modification showed the possibility to control endwall flow and boundary layer loading. Moreover, the favourable influence on the blade load distribution could be observed resulting in the avoidance of the separation region. Although SKE, according to the given definition, has been reduced no general conclusion about the potential improvements can be made here. An optimisation of the shroud endwall may be a more appropriate example for the investigation of that topic due to the by far weaker separation in this region. However, the long-term goal is to derivate qualified design rules for non-axisymmetric endwalls in compressors.

## 6. REFERENCES

[1] Brennan G., Harvey N., Rose M., Fomison N., Taylor M.: “Improving the Efficiency of the Trent 500 HP Turbine Using Non-Axisymmetric End Walls: Part I: Turbine Design”, J. Turbomach., Vol. 125 Issue 3, (2003), pp 497-504.

[2] Harland J., Gregory-Smith D., Harvey N., Rose M.: “Non-Axisymmetric Turbine End Wall Design: Part II – Experimental Validation”, J. Turbomach., Vol. 122 Issue 2, (2000), pp 286-293.

[3] Germain T., Nagel M., Baier R.-D.: ”Visualisation and Quantification of Secondary Flows: Application to Turbine Bladings with 3D-Endwalls”, Paper ISAIF8-0098, (2007).

[4] Vanderplaats G.N.: “Numerical Optimisation Techniques for Engineering Design”, McGraw-Hill, (1984).

[5] Goldberg, D.E.: “Genetic Algorithm”, Addison Wesley (1994).

[6] Demeulenaere A., Hirsch Ch.: ”Application of Multipoint Optimisation to the Design of Turbomachinery Blades”, ASME Paper GT2004-53110, (2004).

[7] Müller M.W., Schiffer H.-P., Hah C.: “Effect of Circumferential Grooves on the Aerodynamic Performance of an Axial Single-Stage Transonic Compressor”, ASME Paper GT2007-27365, (2007)

[8] Müller M.W., Biela C., Schiffer H.-P., Hah C.: “Interaction of Rotor and Casing Treatment in an Axial Single-Stage Transonic Compressor”, ASME Paper GT2008-50135, (2008)

[9] Pierret S., Demeulenaere A., Gouverneur B., Hirsch C.: “Designing Turbomachinery Blades with the Function Approximation Concept and the Navier-Stokes Equation”, AIAA 2000-4879, (2000).

[10] Krose B., van der Smagt P.: “An Introduction to Neural Networks, University of Amsterdam, (1993).

[11] Dorfner C., Nicke E., Voss C.: “Axis-Asymetric Profiled Endwall Design using Multiobjective Optimization Linked with 3D RANS-Flow-Simulation”, ASME Paper GT2007-27268, (2007).